

Dynamics and free energy of α -alumina (0001) surfaces: I. Semi-empirical model

This article has been downloaded from IOPscience. Please scroll down to see the full text article.

2002 J. Phys.: Condens. Matter 14 7797

(<http://iopscience.iop.org/0953-8984/14/34/302>)

View [the table of contents for this issue](#), or go to the [journal homepage](#) for more

Download details:

IP Address: 171.66.16.96

The article was downloaded on 18/05/2010 at 12:25

Please note that [terms and conditions apply](#).

Dynamics and free energy of α -alumina (0001) surfaces: I. Semi-empirical model

A Marmier and M W Finnis¹

Atomistic Simulation Group, School of Mathematics and Physics, Queen's University Belfast, Belfast BT7 1NN, UK

E-mail: m.finnis@qub.ac.uk

Received 17 June 2002

Published 15 August 2002

Online at stacks.iop.org/JPhysCM/14/7797

Abstract

We report an atomistic investigation of static and dynamic properties of the (0001) surface of α -alumina at different temperatures. Lattice dynamics calculations are performed within the quasiharmonic approximation using a periodic slab geometry and with two parametrizations of the shell model. One of our aims is to prepare the ground for a more precise first-principles treatment, by checking the convergence of dynamical properties with respect to slab thickness, vacuum size and k -point sampling. The surface systematically undergoes a large relaxation, and we study the role of surface vibrational modes in the apparent position of the surface plane. An analysis of the mean square displacement of the atoms shows that the amplitudes of vibration of the atoms are 1.5 time larger at the surface than in the bulk. We find that these amplitudes converge slowly with slab thickness, and that the surface modes involve more than just the surface Al atoms. Another aim is to study the surface free energy, which we find has two favourable properties from the point of view of ease of computation. Firstly, we have calculated it for various coarse and fine samplings of phonon wavevectors in the Brillouin zone and find that it can already be well approximated with a sampling of just two k -points. Secondly, the vibrational contribution to the surface free energy converges much faster with respect to slab thickness than the mean square amplitude of vibration. The values of the surface free energy obtained with the two shell models differ by 20% but have similar temperature dependence and bracket the experimental value.

1. Introduction

Alumina surfaces are of great importance for many technological applications. These range from catalysis support, thin-film substrate, dielectrics in microelectronics devices to corrosion

¹ Author to whom any correspondence should be addressed.

and wear protection. Furthermore, α -alumina, as the simplest aluminium oxide and most stable thermodynamically, is a model system for understanding metal oxides.

The study of its surfaces has thus attracted much experimental [1–5] and theoretical [6–13] attention. Even the structure of the simplest clean surface (α -alumina (0001)) has caused some controversy. The last three years have seen many experimental attempts to identify the structure of α -alumina (0001). All the ion scattering [1, 2] and x-ray [2, 3] experiments conclude that the surface is Al terminated although [1] and [3] only considered purely Al- or O-terminated surfaces. A tensor LEED [4] analysis led to a proposed 2:1 mix of Al- and O-terminated terraces as the best model to fit the data. However, a more recent tensor LEED [5] analysis strongly favoured the Al termination. The same conclusion is reached by the most recent ion scattering [2] experiment which also considered mixtures as potential candidates.

On the theoretical side, the conclusions are rather clear, if incomplete: all studies, whether semi-empirical [6, 12, 13] or using different flavours of *ab initio* Hartree–Fock (HF) [7] or based on the density functional theory (DFT) [8–11] identify the Al-terminated surface as being the most stable. The most recent DFT work includes the effect of the environment, namely by taking into account the effect of water [8], hydrogen [11] or oxygen [10]. In all cases, an Al-terminated surface remains the most stable except at oxygen partial pressures exceeding an atmosphere.

Whereas there are good reasons to believe that the surface is normally terminated by a single aluminium layer, which relaxes strongly inwards, the degree of relaxation experienced by the different atomic planes is far from being resolved. Most experiments and all theoretical works agree on the direction of relaxation of the outer Al plane (with the exception of [4]). The discrepancy lies in the amount of relaxation. Experiments obtain inward relaxations of 50–60% for the outermost Al layer, whereas theoretical studies suggest something near 70–80%. Even those DFT calculations which take into account some effect of the environment [8, 10, 11] have not removed this discrepancy with experiments concerning the amount of relaxation.

In line with the interpretation of tensor LEED data, it has recently been suggested [5] that the presence of a soft surface vibrational mode could explain the discrepancy. Information about the dynamics of α -alumina (0001) [12, 13] is scarce and details about the surface modes are not reported. One of our motivations was therefore to study the surface dynamics in sufficient detail to decide whether a soft surface mode could be responsible for the reduced relaxation as measured experimentally. Furthermore, a calculation of the vibration spectrum gives us the vibrational contribution to the free energy, at least within the quasiharmonic approximation. This is another reason to investigate the dynamics of α -alumina (0001) with both semi-empirical potentials and then with a more reliable first-principles description.

In the present investigation, quasiharmonic lattice dynamics (QHL) is used in conjunction with two different semi-empirical models. We are aware of two previous theoretical studies of the dynamics of the α -alumina surface, namely [12], using QHL with a shell model and [13], using molecular dynamics (MD) and a shell model. The QHL study focuses on the temperature dependence of the free energy and relaxations of the surface but does not discuss the amplitude of the ionic displacements. The MD work reports the mean square displacements (MSD), but does not discuss individual surface modes or the contribution of vibrational entropy to the surface free energy. We extend the scope of these previous studies and our purpose is somewhat different. At least at reasonably low temperature (typically half the melting temperature, of 2288 K for alumina), QHL allows a more detailed description of the dynamics than MD, as the displacement of the atoms for each mode are accessible (via the eigenvectors of the dynamical matrix) and the computation of the free energy including quantum vibrational effects is straightforward. Secondly, QHL provides a convenient framework for testing the convergence of phonon-related properties with respect

Table 1. Parameters of the shell models.

	Model 1			Model 2		
	A (eV)	ρ (Å)	C (eV Å ⁻⁶)	A (eV)	ρ (Å)	C (eV Å ⁻⁶)
Al _s -O _s	1 460.3	0.299	0.00	1 474.4	0.3006	0.00
O _s -O _s	22 764.3	0.149	27.88	22 764.3	0.1490	20.37

	Model 1		Model 2		
	Q_s (e)	k_1 (eV Å ⁻⁴)	Q_s (e)	k_1 (eV Å ⁻²)	k_2 (eV Å ⁻⁴)
Al	1.3830	98.829	1.458	1732.00	0.0
O	-2.8106	103.07	-3.000	60.78	10 000.0

to slab parameters (thickness, vacuum size) and to vibrational k -point sampling. Thus, by studying the convergences in real as well as in k -space, we prepare the ground for more accurate first-principles density functional calculations, the results of which we will report in a subsequent paper.

2. Methods

2.1. Alumina

Alumina has the corundum structure, i.e. has rhombohedral space group $R\bar{3}C$, with two formula units per primitive cell. The material is commonly described in terms of a hexagonal structure with six formula units per unit cell, which is especially convenient for studying its (0001) surface. It can also be viewed as a stacking of alternating O and Al planes along the (0001) direction, according to the sequence AlO₃Al-AlO₃Al, where the oxygens in each group of three are coplanar. We used the following experimental [14] lattice parameters as a first guess for our calculation: $a = 5.1284$ Å and $\alpha = 55.28$ (corresponding in the hexagonal structure to $a = b = 4.7589$ Å and $c = 12.991$ Å). The slab that we used for the surface calculation consisted of a stack of up to 12 stoichiometric AlO₃Al groups of planes, separated by a vacuum of between 12 and 40 Å. Periodic boundary conditions are applied in directions parallel to the surfaces of the slab.

2.2. Interatomic potentials

We have applied two sets of shell model parameters which have been used in recent simulations concerned with the dynamical properties of α -alumina (0001) bulk [15] and surface [13]. These models like other empirical potentials are known to stabilize the bixbyite structure instead of the experimental corundum structure for bulk alumina; nevertheless, their description of the structure of the (0001) surface is comparable to *ab initio* results. These shell models consist of a short-range repulsion between ions of the Buckingham form ($V(r) = A \exp(-\rho/r) - C/r^6$), together with a long-ranged Coulomb interaction between ions. The polarizability is accounted for by a shell of charge Q_s displaced by a distance r from a core of charge $Q_c = Z - Q_s$ (Z being the total ionic charge). The core and the shell are attached by a spring of potential energy: $V(r) = \frac{1}{2}k_1r^2 + \frac{1}{24}k_2r^4$. The parameters for the two models are given in table 1.

Table 2. Hexagonal bulk cell lattice parameters.

T (K)	Model 1		Model 2	
	a (Å)	c (Å)	a (Å)	c (Å)
0	4.7892	12.5366	4.8383	12.7612
300	4.7913	12.5423	4.8399	12.7655
600	4.7970	12.5573	4.8452	12.7795
900	4.8037	12.5747	4.8518	12.7969
1200	4.8110	12.5939	4.8591	12.8162
1500	4.8189	12.6144	4.8669	12.8368

2.3. Lattice dynamics

In the quasiharmonic approximation the Helmholtz free energy is given by

$$F(V, T) = E(V) + \sum_{\mathbf{q}, j} f_j(\mathbf{q}) \quad (1)$$

$$f_j(\mathbf{q}) = \frac{1}{2} h \nu_j(\mathbf{q}) + kT \ln[1 - \exp(-h \nu_j(\mathbf{q})/kT)]$$

where $E(V)$ is the potential energy of the static lattice at a volume V and $f_j(\mathbf{q})$ is the vibrational contribution of the j th mode at wavevector \mathbf{q} with a frequency $\nu_j(\mathbf{q})$. Anharmonic effects are included through the explicit volume dependence of the potential energy.

All calculations are performed with the program GULP [16].

We used the following strategy. First, we optimized the hexagonal bulk structure (containing 30 atoms) at various temperatures, the internal coordinates and the lattice parameters being allowed to relax at this stage in order to minimize F . Then, for each temperature, a slab was generated with the lattice parameter obtained previously. For this, only the internal coordinates are allowed to relax. At each stage, a maximum number of $(12 \times 12 \times 1)$ k -points were used for the summation of the vibrational contributions to the free energy.

This would be rather a cumbersome procedure to carry out using a DFT method, because the thermal expansion has to be calculated in an iterative manner. It is therefore of interest to see how well a purely harmonic approximation will work. In this case the volume of the cell is not allowed to relax, and the internal coordinates are determined by relaxing not the free energy but the internal energy calculated with the static lattice.

3. Results and discussion

3.1. Bulk

The calculated lattice parameters for the hexagonal bulk structure at different temperatures are given in table 2. At 301 K, the lattice parameters of model 1 are 0.7% bigger than the experimental value, and 1% bigger for model 2. The thermal expansion (perpendicular to the c -axis) coefficients are $4.9 \times 10^{-6} \text{ K}^{-1}$ for model 1 and $4.7 \times 10^{-6} \text{ K}^{-1}$ for model 2, comparable to the experimental value, variously quoted between 5.9 and $6.9 \times 10^{-6} \text{ K}^{-1}$ [17]. The quality of the calculated dynamics can be tested first on the bulk dispersion curves. These are known experimentally [18] (neutron scattering) and have been recently calculated [19].

The calculated dispersion curves at 301 K for these two models are shown in figures 1(a) and (b). They reproduce most of the features of the experimental ones. The range of frequencies at various symmetry points compares especially well, for both models.

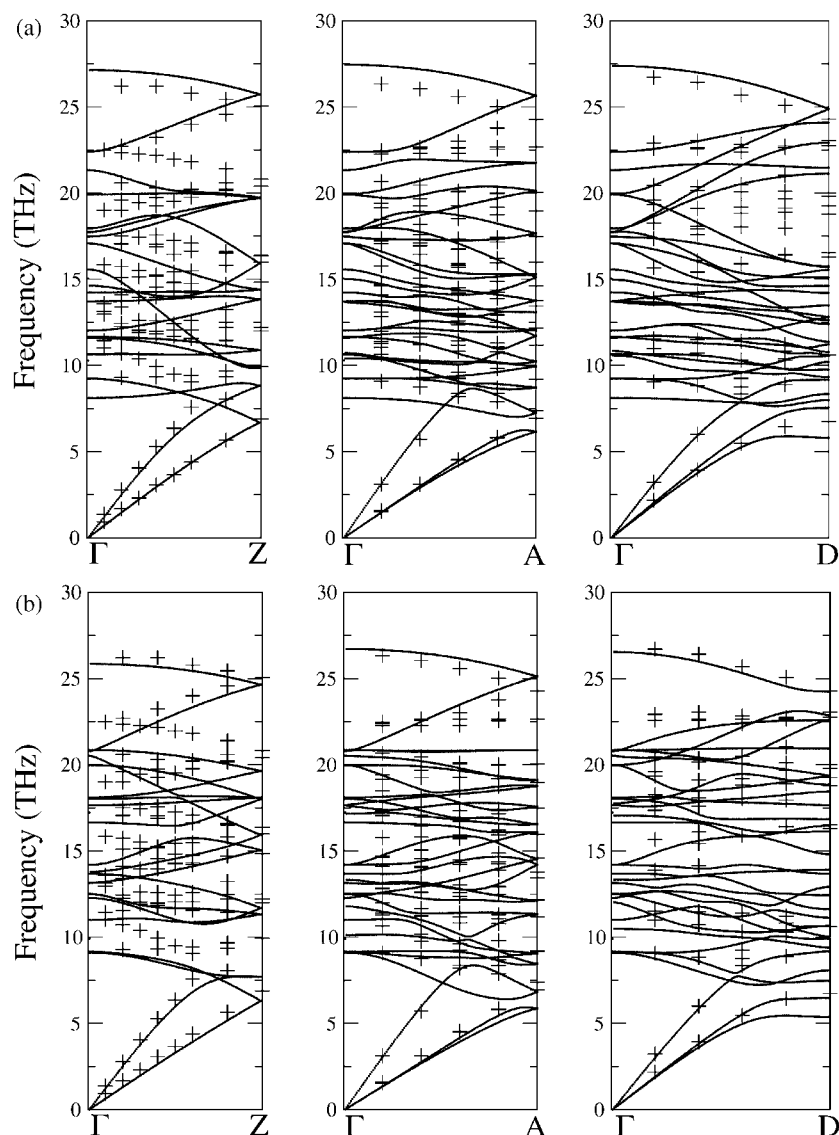


Figure 1. Bulk α -alumina dispersion curves at 301 K along directions of high symmetry for shell (a) model 1 and (b) model 2. The crosses represent the neutron scattering value from [18].

3.2. Surface structure

As expected, the surface undergoes a strong relaxation. The relaxations of each layer are summarized in table 3. Table 3(c) shows that previous calculations span a broad range of relaxations. With the exception of [4], all results are at least in the same direction. The distance between the outermost Al atoms and the first O plane is greatly reduced (with respect to the bulk value), by at least 50% according to most experiments, and up to 85% for DFT calculations. The magnitude of the relaxation between the first O plane and the second Al plane is much smaller and there is no clear trend. The experimental data become less plentiful

Table 3. Relaxations of Al-terminated surfaces (per cent of the relevant bulk spacing), for model 1 (a), model 2 (b) and other work (c).

(a)					
T (K)	Al ₁ O ₁	O ₁ Al ₂	Al ₂ Al ₃	Al ₃ O ₂	O ₂ Al ₄
0	-56.4	7.2	-44.3	23.8	6.5
300	-56.9	6.9	-44.2	23.7	6.5
600	-57.9	6.3	-44.2	23.8	6.7
900	-59.7	5.2	-44.3	23.9	7.1
(b)					
T (K)	Al ₁ O ₁	O ₁ Al ₂	Al ₂ Al ₃	Al ₃ O ₂	O ₂ Al ₄
0	-73.9	12.1	-41.5	26.5	11.3
300	-73.9	12.0	-41.6	26.6	11.5
600	-74.4	11.2	-41.4	26.5	11.8
900	-75.1	10.3	-41.0	26.4	12.0
(c)					
Method	Al ₁ O ₁	O ₁ Al ₂	Al ₂ Al ₃	Al ₃ O ₂	O ₂ Al ₄
X-ray [3]	-51	16	-29	20	—
TOF-SARS [1]	-63	—	—	—	—
LEED [4]	30	6	-55	—	—
Tensor LEED [5]	-50.0	6.3	—	—	—
HF [7]	-78.8	-3.7	-43.6	7.9	—
GGA [8]	-85	3	-45	20	—
GGA [11]	-86	6	-49	22	6
GGA (with H) [11]	-69	—	—	—	—
GGA [9]	-69.6	10.4	-34.3	18.5	3.4
Shell, MD [13]	-58	4	-42	24	—

for the deeper layers, but there still seems to be a discrepancy for the Al₂–Al₃ distance, where calculations predict a relaxation of around 50% and x-ray results only 30% (interlayer distance of 0.32 and 0.46 Å, compared to the bulk value of 0.63 Å). Tables 3(a) and (b) show the relaxations, as calculated with the two shell models. The relaxations obtained with model 2 are larger than with model 1. Model 1 gives the results which seem more compatible with the experimental ones. The influence of the temperature is quite marginal.

3.3. Surface dynamics

3.3.1. Surface modes. The study of the eigenvectors of the dynamical matrix of the slab shows that the modes which exhibit a surface character, i.e. where the displacements in a large central part of the slab are negligible compared to those near the vacuum, all involve the significant motion of the atoms of at least two AlO₃Al groups of planes, as can be seen in figure 2. Among these modes, those where the motion of the atom is predominantly perpendicular to the surface have a frequency below 10 THz (300 cm⁻¹ or about 450 K) for both shell models. We have not found a mode so localized that only the outermost Al atoms move significantly with either of these shell models. This result is not compatible with the assumption of the last tensor LEED analysis [5]. It was shown that in order to best model the experimental data, a ‘split Al atom’ had to be used to model the terminating Al layer. In this model, a mixture of two domains was considered, allowed to relax separately in order to fit the data. The difference in the position of the Al atoms in the two domains is related to the vibrational amplitude.

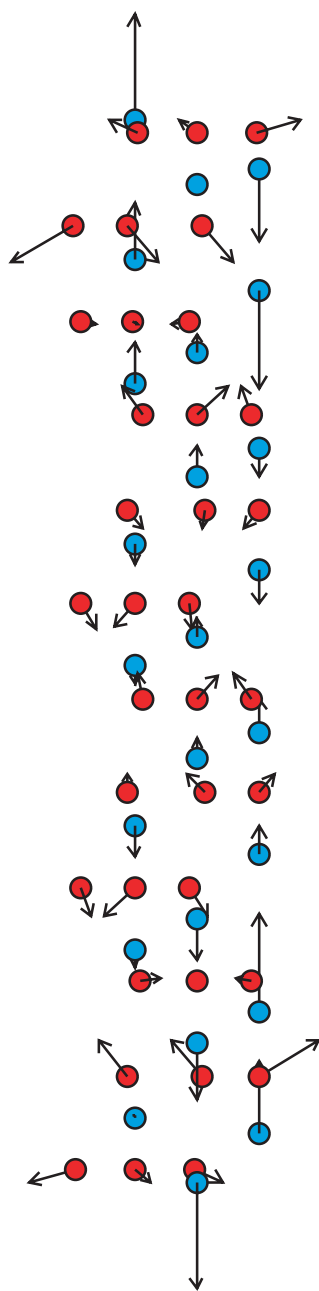


Figure 2. The phonon mode with the most pronounced surface localization.
(This figure is in colour only in the electronic version)

The observed difference is 0.14 \AA , and was interpreted as an indication of a strong anharmonic localized vibrational mode. We consider that this interpretation of surface relaxations requires surface modes to be both localized on the terminating Al layer and anharmonic which is not compatible with our present results.

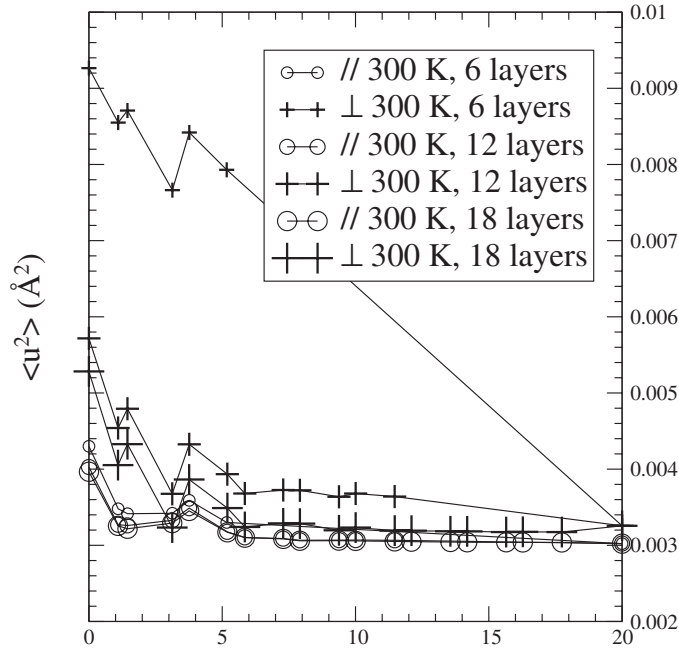


Figure 3. MSDs of the Al atom for different slab thicknesses as a function of atom depth in the slab for shell model 1.

3.3.2. Mean squared displacement. We can analyse the dynamics of the slab in terms of MSDs, calculated from the eigenvectors of the dynamical matrix as in [20]:

$$\langle u_{i\alpha}^2 \rangle = \frac{1}{2M_i} \sum_{q,j} w(\mathbf{q}) A_j^2(\mathbf{q}) e_{ji\alpha}^2(\mathbf{q}), \quad (2)$$

where $u_{i\alpha}$ is the displacement along direction α of the i th atom, M_i its mass, $e_{ji\alpha}$ the coordinate (corresponding to this atomic displacement) of the dynamical matrix eigenvector associated with the j th modes at wavevector \mathbf{q} , w the weight associated to wavevector \mathbf{q} and $A_j(\mathbf{q})$ the amplitude of this mode given by Bose–Einstein statistics:

$$A_j^2(\mathbf{q}) = \left(\frac{2}{\exp(h\nu_j(\mathbf{q})/kT) - 1} + 1 \right) \frac{h}{4\pi^2\nu_j(\mathbf{q})}. \quad (3)$$

We found that in order to obtain good convergence (MSD at the centre of the slab differing by less than 10% from its value in the bulk at 300 K), a slab of 12 AlO_3Al groups of planes was necessary. This can be seen in figure 3, where the MSDs of the Al atoms as a function of their depth in the slab are plotted for slabs of 6, 12 and 18 AlO_3Al groups of planes for shell model 2 at 300 K. The component of the MSD parallel to the surface converges very fast, but the thinnest thin slabs give totally wrong values for the perpendicular component. We discuss this at first glance somewhat surprising behaviour in section 3.3.4.

At 350 K (the temperature used in [5]), we find that the two models give very similar values for the root mean squared displacement (RMSD) of the Al atom in the bulk, namely 0.102 and 0.099 \AA respectively. For a simple harmonic oscillator the RMSD is related to its amplitude by a factor $1/\sqrt{2}$; these values thus correspond to amplitudes of 0.144 and 0.140 \AA , in good agreement with the value of 0.12 \AA from [5] estimated from the Debye temperature derived from LEED calculations.

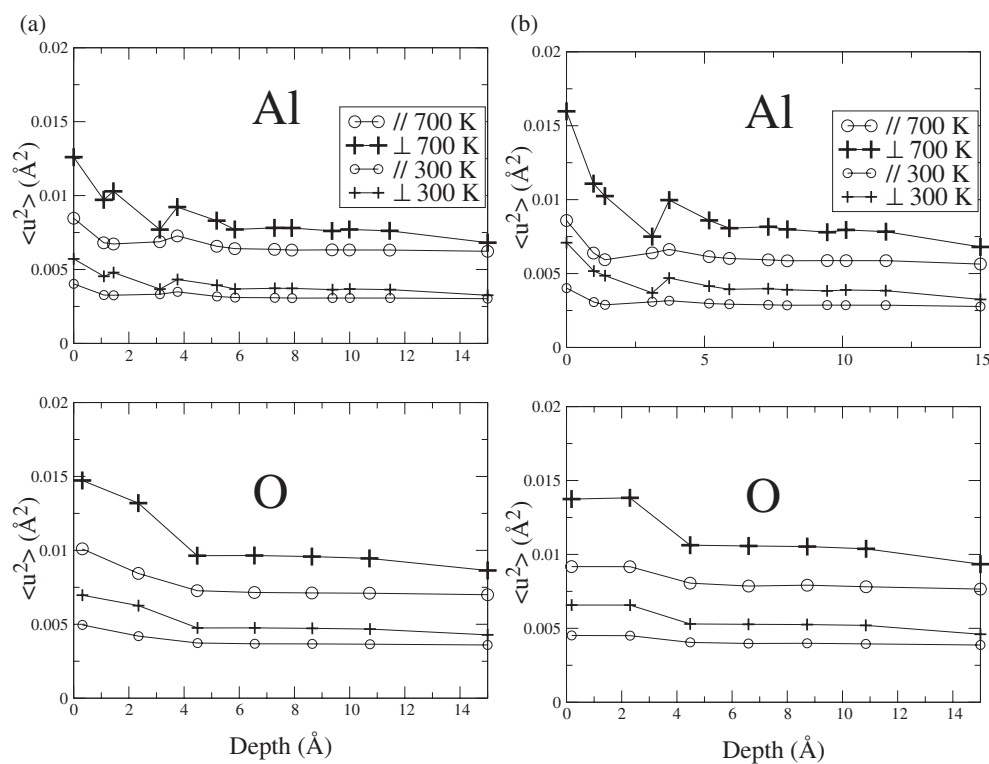


Figure 4. MSDs as a function of atom depth in the slab for shell (a) model 1 and (b) model 2.

The MSDs of atoms as a function of their depth in the slab are plotted in figure 4. We have separated the two models, but also the two types of atom and the contributions to the MSD perpendicular and parallel to the surface. The latter quantity has been averaged over displacements along the x - and y -directions. The sets of curves for the two different models exhibit striking similarities, with the notable exception of the perpendicular motion of the surface Al atom, larger in model 2 than in model 1. Whereas these curves, especially concerning the value of the MSD of the surface atoms, are very similar to those obtained with MD [13] (with model 2), our bulk displacements are roughly 30% larger. We have no explanation for this discrepancy.

For the surface Al atom in model 1, the RMSD perpendicular to the surface at 300 K is 0.076 \AA , 32% more than in the bulk (0.057 \AA). In the case of model 2, this quantity reaches 48% (0.084 \AA for the surface Al atom, compared to 0.057 \AA for bulk Al atoms).

3.3.3. Free energy. We have found only one previous calculation of the (0001) surface free energy (see [12]). It was shown there that the surface free energy depends significantly on the potential used, ranging from 1.6 to 3.2 J m^{-2} at 0 K, whereas the decrease of the surface energy with temperature shows less of an absolute difference between the potentials, the total variation of free energy with temperature being around -0.18 J m^{-2} over the range 0–1500 K. Calculated values of the surface energy without the vibrational contribution are quite numerous. We are also aware of one calorimetric experiment [21] measuring this quantity as 2.6 J m^{-2} . Most theoretical values lie between 2.0 and 3.0 J m^{-2} (see for instance table 3 in [13]). The surface

Table 4. Convergence of the surface free energy (J m^{-2}) with respect to the size of the vacuum (a), number of layers (b) and BZ sampling for model 1 (c) and model 2 (d).

(a)					
Vacuum size	Model 1 (301 K)	Model 2 (301 K)			
0.5	2.8896	2.4345			
1	2.8939	2.4381			
2	2.8939	2.4380			
3	2.8940	2.4380			
(b)					
Number of layers	Model 1 (301 K)	Model 2 (301 K)			
4	2.8823	2.4397			
5	2.8831	2.4571			
6	2.8939	2.4381			
12	2.9035	2.4474			
(c)					
Type of sampling	0 K	300 K	600 K	900 K	
Γ	2.9302	2.9045	2.8624	2.8189	
$\Gamma + 3X$	2.9210	2.8965	2.8504	—	
MP 12	2.9193	2.8939	2.8466	2.7952	
(d)					
Type of sampling	0 K	300 K	600 K	900 K	1200 K
Γ	2.4636	2.4422	2.4149	2.3886	2.3617
$\Gamma + 3X$	2.4575	2.4404	2.4143	2.3882	2.3602
MP 12	2.4562	2.4381	2.4104	2.3824	2.3524

energies that we obtain with shell models 1 and 2 are 2.951 and 2.454 J m^{-2} respectively. The influence of the zero-point energy is quite small and rather subtle. For shell model 1, the surface free energy at 0 K is 2.92 J m^{-2} whereas for model 2, the surface free energy at 0 K is 2.456 J m^{-2} , and therefore is almost identical to the static surface energy. The convergence of the surface free energy with respect to the number of layers, the size of the vacuum and the sampling of the Brillouin zone is summarized in table 4.

A slab containing six $\text{Al-O}_3\text{-Al}$ groups of planes leads to values of the surface free energy differing by less than 0.5% (at 300 K) from that obtained with a slab twice as thick. Surprisingly, very thin slabs of five or even four groups of planes also give precise values of the surface free energy ($<1\%$ difference at 300 K). The slab vibrational contribution to the surface free energy is 0.141 and 0.145 J m^{-2} for slabs of thickness 6 and 18 layers respectively, in the case of shell model 1 at 300 K .

For the vacuum separating the periodic images of the slab, we find that a gap equal to the slab thickness is sufficient for converging the surface free energy.

The shell models used here are sufficiently simple to allow a highly accurate sampling of the vibrational Brillouin zone. Other methods, such as supercell DFT, do not allow us this luxury. It is therefore important to check whether or not a limited sampling allows a satisfactory computation of the free energy. We also want to check the influence of using a simplified version of the harmonic approximation, in which we not only neglect the thermal expansion of the cell but also relax its internal coordinates following the gradient of the static energy instead of the free energy.

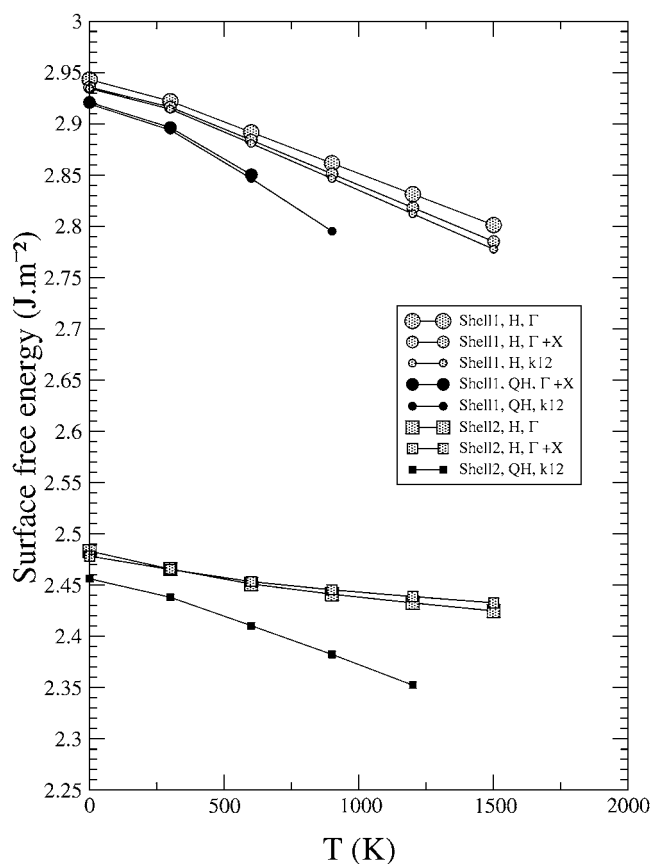


Figure 5. Surface free energy as a function of temperature.

From tables 4(c) and (d) we deduce that using only the Γ point, with model 1 we predict the vibrational contribution to the free energy at 600 K with an error of 22%, and with model 2 the error is 10%. We refer here to just the sampling errors. By using two k -points, namely Γ and X, instead of only Γ , the error for model 1 is reduced to 5.2% and for model 2—8.5%. In view of the other uncertainties in the free energy, these results suggest that the sampling with two k -points is adequate.

In figure 5 we plot the evolution of the surface free energy with temperature, for the two models and for two different strategies. The first one consists in using the quasiharmonic approximation, with high-precision k -sampling: it leads to the most precise results that we can achieve. The second one uses the harmonic approximation with a crude sampling, corresponding to what it would be feasible to calculate with DFT with minimum computational effort. With both models the harmonic approach overestimates the surface energy by around 1% at 301 K. It also leads to underestimation of the slope of the $F(T)$ curves. The two models differ in the temperature dependence of the free energy, the decrease being more pronounced for model 1, 0.12 J m^{-2} between 0 and 900 K, compared to only 0.08 J m^{-2} in the case of model 2. As the thermal expansion coefficients are very similar, this difference can only be explained by differences in the details of the dispersion curves of the slabs. Indeed, the slab dispersion curves (not shown here) at high frequency tend to be very similar to their bulk equivalent for model 1, but to reach a higher frequency for model 2. For comparison,

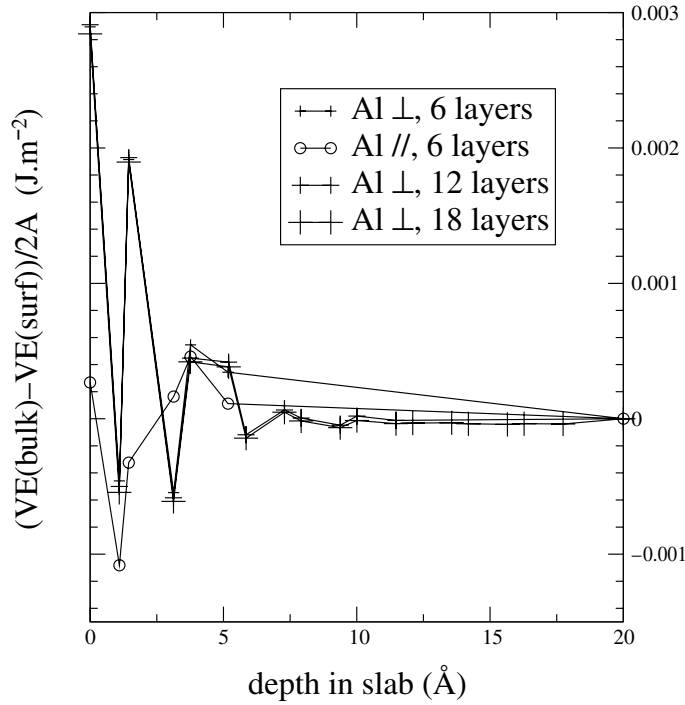


Figure 6. The projected surface free energy for the motion perpendicular to surface of Al atoms for different slab thicknesses as a function of atom depth in the slab (shell model 1).

the potentials of [12] lead to decreases between 0.11 and 0.14 J m^{-2} over the same range of temperature. This decrease is clearly quite strongly model dependent.

3.3.4. Convergence with slab thickness. In order to understand why the free energy converges already for thin slabs whereas these lead to very wrong values for the MSD, we project the vibrational part of the free energy (including the zero-point energy) onto the individual atomic displacements according to

$$F_{i\alpha} = \sum_{q,j} f_j(\mathbf{q}) w(\mathbf{q}) e_{ji\alpha}^2(\mathbf{q}). \quad (4)$$

We plot the surface free energy corresponding to the displacement of the Al atom perpendicular to the surface in figure 6 for shell model 1 at 300 K. Like the MSD, the ‘projected’ free energies are summations over the mode index and the k -points of the squares of the components of the corresponding eigenvector weighted by a function depending explicitly on the frequency. Despite this formal similarity, the perpendicular components of this projected surface energy for the Al atoms are well converged for a thin slab of six AlO_3Al groups of planes.

A frequency decomposition of the MSD and ‘projected’ free energies (not presented here) shows that it is the *lowest*-frequency modes that are responsible for an additional contribution to the projected MSD (see figure 3) which is strongly dependent on the slab thickness but *not* on the depth within a slab. It is also a contribution which increases as the k -point sampling is made finer. This is a direct consequence of the fact that the absolute MSD diverges for a two-dimensional crystal, or slab (for a good discussion on this subject see appendix D of [23]).

In practical calculations the long-wavelength limit which is responsible for the divergence may be hidden by the discrete sampling, but it always emerges when the sampling is made finer or when the slab is thin enough. As the slab thickness increases, and acquires a more and more pronounced bulk character (or equivalently the relative importance of the acoustic modes responsible for the divergence is reduced), the MSD appears to converge better. Fortunately, the MSD appropriate to a semi-infinite crystal can still be extracted with confidence from thin-slab calculations by the simple trick of measuring the displacements with respect to the displacement of an atom at the centre of the slab. By applying this procedure, the MSD perpendicular to the surface of the outermost Al atom differs by 14% when calculated for slabs of 6 and 18 groups of planes and by 0.5% for 12 and 18 groups of planes.

4. Conclusions

We have investigated static and dynamic properties and calculated the surface free energy of alumina slabs for a range of temperature using two shell models.

Shell model 1 leads to surface relaxations in good agreement with recent experimental results, in better agreement than either shell model 2 or published *ab initio* results. The effect of surface anharmonicity is not important here. The prominent feature of this model is the relatively strong polarizability of the Al³⁺ ion (0.2783 Å³ for model 1, 0.0176 Å³ for model 2, which may be compared with 0.79 Å³ extracted experimentally [24]). However, there still seems no reason to believe that model 1 should be more realistic than *ab initio* calculations.

It may also be that the discrepancy between experimental and theoretical relaxations is due more to the effect of the environment than to the surface dynamics, and it would also be hazardous to conclude that shell model 1 describes the surface significantly better than shell model 2.

The MSDs obtained by QHLD agree with those from previously published MD calculations at the surface, but discrepancies remain with the bulk calculations.

The modes which exhibit a 'surface' character are not localized on the outermost Al atoms, but involve significant motion of the atoms of the outer two AlO₃Al groups.

This does not support the hypothesis of [5], where it is suggested that a mode essentially localized on the outermost Al atoms is responsible for the noted discrepancy between experimental and theoretical relaxation. Preliminary DFT [22] results show that the surface modes are more strongly localized on the outer Al atoms than predicted by the shell models, and this question will be revisited.

The free energies calculated with the two models differ by 20%. They decrease with temperature, at a rate depending on the model.

Finally we show that even just a two-*k*-point sampling of the vibrational Brillouin zone in the slab geometry gives well converged results for the free energy and MSD of a surface. The MSDs must be measured with respect to atoms at the centre of the slab; otherwise they are divergent in principle for any finite slab thickness. For the free energy, six groups of AlO₃Al planes are adequate. The MSDs converge rather less well than the free energy, but are well converged with 12 groups of planes. These results are particularly important in showing that the computation of the free energy is achievable by means of supercell *ab initio* methods with cells of just 60 atoms.

References

- [1] Ahn J and Rabalais J W 1997 *Surf. Sci.* **388** 121
- [2] Suzuki T, Hishita S, Oyoshi K and Souda R 1999 *Surf. Sci.* **437** 289

-
- [3] Guenard P, Renaud G, Barbier A and Gautier-Soyer M 1998 *Surf. Rev. Lett.* **5** 321
 - [4] Toofan J and Watson P R 1998 *Surf. Sci.* **401** 162
 - [5] Walters C F, McCarthy K F, Soares E A and Van Hove M A 2000 *Surf. Sci.* **464** L732
 - [6] Mackrodt W C, Davey R J and Davey S N 1987 *J. Cryst. Growth* **80** 441
 - [7] Gomes J R B, Moreira I de P R, Reinhard P, Wander A, Searle B G, Harrison N M and Illas F 2001 *Chem. Phys. Lett.* **341** 412
 - [8] Di Felice R and Northrup J E 1999 *Phys. Rev. B* **60** R16 287
 - [9] Batirev I G, Alavi A, Finnis M W and Deutsch T 1999 *Phys. Rev. Lett.* **82** 1510
 - [10] Batirev I G, Alavi A and Finnis M W 2000 *Phys. Rev. B* **62** 4698
 - [11] Wang X G, Chaka A and Scheffler M 2000 *Phys. Rev. Lett.* **84** 3650
 - [12] Simms C E 1999 *PhD Thesis* University of Bristol
 - [13] Baudin M and Hermansson K 2001 *Surf. Sci.* **474** 107
 - [14] Lee W E and Lagerlof K P D 1985 *J. Electron Microsc. Tech.* **2** 247
 - [15] Rambaut C, Jobic H, Jaffrezic H, Kohanoff J and Fayeulle S 1998 *J. Phys.: Condens. Matter* **10** 4221
 - [16] Gale J D 1997 *J. Chem. Soc. Faraday Trans.* **93** 629
 - [17] Landolt-Börnstein 1971 Group II, vol 1 (Berlin: Springer) p 586
 - [18] Schober H, Strauch D and Dorner B 1993 *Z. Phys. B* **92** 273
 - [19] Heid R, Strauch D and Bohnen K-P 2000 *Phys. Rev. B* **61** 8625
 - [20] Maradudin A A, Montroll E W and Weiss G H 1963 *Solid State Physics Supplement 3* (New York: Academic)
 - [21] McHale J M, Auroux A, Perrota A J and Navrotsky A 1997 *Science* **277** 788
 - [22] Marmier A and Finnis M W 2002 to be published
 - [23] Allen R E and De Wette F W 1969 *Phys. Rev.* **179** 873
 - [24] Shannon R D 1993 *J. Appl. Phys.* **73** 348